https://doi.org/10.5194/egusphere-2024-1519
Preprint. Discussion started: 24 May 2024

The impact of coupled 3D radiative transfer on surface radiation and cumulus clouds over land

Mirjam Tijhuis[1], Bart J. H. van Stratum[1], and Chiel C. van Heerwaarden[1]
[1]Meteorology and Air Quality Group, Wageningen University & Research, Wageningen, the Netherlands
Correspondence: Mirjam Tijhuis (mirjam.tijhuis@wur.nl)

Abstract. Radiative transfer is a 3D process, but most atmospheric models consider radiation only in the vertical direction for computational efficiency. This results in inaccurate surface radiation fields, as the horizontal transport of radiation is neglected. Previous work on 3D radiative effects mainly used 3D radiative transfer uncoupled from the flow solver. In contrast, our current work uses 3D radiative transfer coupled to the flow solver to study its impact on the development of clouds and the resulting impact on the domain-averaged surface solar irradiance. To this end, we performed a series of realistic Large-Eddy simulations with MicroHH. To improve the level of realism of our radiation, we first included the direct effect of aerosols using aerosol data from the CAMS global reanalysis. Next, we performed simulations with 1D radiative transfer and with a coupled ray tracer, for 12 days on which shallow cumulus clouds formed over Cabauw, the Netherlands. In general, simulations with the coupled ray tracer have a higher domain-averaged liquid water path, larger clouds, and similar cloud cover compared to simulations with 1D radiative transfer. Furthermore, the domain-averaged direct radiation is decreased with 3D radiative transfer and the diffuse radiation is increased. However, the average difference in global radiation is less than 1 W m^{-2}, as the increase in global radiation from uncoupled 3D radiative transfer is counterbalanced by a decrease in global radiation caused by changes in cloud properties.

1 Introduction

Radiative transfer is a 3D process, which is often reduced in atmospheric models to a 1D process for computational efficiency. Previous work has shown that this 1D approximation leads to errors in cloud-resolving models, as it neglects the horizontal transport of radiation (e.g., Várnai and Davies, 1999; Cahalan et al., 2005; Gristey et al., 2020a). As a result, cloud-resolving simulations with 1D radiation have brighter cloud shadows than simulations with 3D radiation, with cloud shadows that are always positioned directly underneath the clouds. In addition, simulations with 1D radiation do not capture cloud enhancements, which are peaks in surface radiation that exceed the clear sky radiation. These differences in surface radiation are relevant for multiple processes, such as renewable energy production (e.g., Kreuwel et al., 2020) and photosynthesis (e.g., Kanniah et al., 2012; Vilà-Guerau de Arellano et al., 2023). Furthermore, the differences in radiation can have an impact on the development of clouds, mainly caused by differences in radiation at the surface and the corresponding differences in surface heat fluxes (Veerman et al., 2022, 2020; Jakub and Mayer, 2017). This impact of 3D radiation on clouds can only be captured when the results of the radiative transfer calculations impact the surface and atmosphere, thus when 3D radiative transfer is coupled to

https://doi.org/10.5194/egusphere-2024-1519
Preprint. Discussion started: 24 May 2024

the flow solver in simulations with an interactive land-surface. As it recently became possible to do Large-Eddy Simulations (LES) with coupled 3D radiation (Veerman et al., 2022; Jakub and Mayer, 2015), we now have the opportunity to investigate the impact of coupled 3D radiative transfer on clouds and surface radiation. Therefore, this paper systematically compares the influence of coupled 1D and 3D radiation on surface radiation and clouds.

Previous studies with 3D radiative transfer that was not coupled to the flow solver (i.e. uncoupled 3D radiative transfer) showed that including the 3D radiative effect is essential to model the correct spatial distribution of shortwave radiation at the surface, including cloud enhancements (Gristey et al., 2020a; Tijhuis et al., 2023). In addition, Gristey et al. (2020a) showed that uncoupled 3D radiative transfer changes the domain-averaged shortwave radiation compared to 1D radiation. The differences between 1D and uncoupled 3D radiative transfer can be explained by two opposing changes. On the one hand, the direct radiation is reduced as the cloud shadow area increases (side illumination, Hogan and Shonk (2013)). On the other hand, the diffuse radiation at the surface increases because radiation escapes from the sides of clouds (Hogan and Shonk, 2013; Várnai and Davies, 1999) and radiation gets entrapped between cloud layers and between the clouds and the surface (Hogan et al., 2019). Uncoupled 3D radiative transfer has also previously been used for the validation of several approximations of 3D radiative transfer (Gristey et al., 2020b, 2022; Wissmeier et al., 2013; Wapler and Mayer, 2008; Jakub and Mayer, 2015; Hogan et al., 2016).

The differences in the domain-averaged surface shortwave radiation and its spatial distribution will impact the development of the clouds, which can only be captured with coupled 3D radiation. So far, the impact of cloud shadows on the development of clouds has mainly been shown with idealized cases (e.g., Gronemeier et al., 2017; Lohou and Patton, 2014; Horn et al., 2015; Schumann et al., 2002). These studies have demonstrated that cloud shadows and their position relative to the cloud influence the cloud development, depending on multiple factors such as solar zenith angle and background wind speed. In addition to the 3D effects in the shortwave spectral range, the 3D effects in the longwave spectral range also influence the clouds (Schäfer et al., 2016; Klinger et al., 2017). An example of how coupled 3D radiation can influence clouds is provided by Jakub and Mayer (2017), who demonstrated that coupled 3D radiative transfer impacts the formation of idealized cloud streets for a range of background winds, solar zenith and azimuth angles. In addition, Veerman et al. (2020) and Veerman et al. (2022) showed for realistic cases of shallow cumulus clouds that coupled 3D radiation results in larger and thicker clouds, but these results are based on single case studies.

We aim to systematically investigate the impact of coupled 3D shortwave radiative transfer on the mean surface radiation and the development of clouds. To this end, we use an LES model (MicroHH, van Heerwaarden et al. (2017)) with interactive land surface and a coupled ray tracer for the shortwave radiation. We focus on cumulus clouds, as they cause large variability in surface radiation and are strongly coupled to the surface. First, we implemented aerosol optics in our radiative transfer solver to reduce a systematic bias in the surface radiation partitioning caused by the absence of aerosols in the radiation model. To validate the inclusion of aerosols, we performed simulations for a set of days with clear skies over Cabauw, the Netherlands, which we compared with observations. Next, we used the setup with aerosols to simulate a set of 12 days during which shallow cumulus clouds developed. After comparing the results with observations to ensure that the simulations resemble reality, we used these simulations to study the impact of coupled 3D radiative transfer on cloud properties and surface direct, diffuse, and

https://doi.org/10.5194/egusphere-2024-1519
Preprint. Discussion started: 24 May 2024

global radiation. To understand the impacts of coupled 3D radiative transfer better, we also investigate the impact of uncoupled 3D radiative transfer, and we examine how the changes in cloud properties feed back to the surface radiation.

2 Methods

2.1 Case selection

For this study, we selected two sets of cases: one set with clear sky days to test our implementation of the aerosol optics and one set with cumulus days to study the impact of coupled 3D radiative transfer. To select the cases, we used the dataset of Mol et al. (2023), which provides ten years of solar irradiance observations in Cabauw, together with, among others, a classification of the weather (clear-sky, variable, overcast) and the satellite-derived cloud type (for the years 2014-2016). Using this dataset, we first selected 13 clear sky days. We chose to use clear sky days to validate our aerosol implementation, as it allows for a direct comparison between observations and our simulations, which is not possible for cloudy days because of the stochastic nature of the clouds. From the days with at least half of the day classified as clear sky, we manually selected 13 days which cover all wind directions and a range of aerosol optical depths (0.015-0.5) that covers all values that are generally found for Cabauw (van Heerwaarden et al. (2021), their figure 3c). Next, we selected 12 days with cumulus clouds. We selected the days in the period 2014-2016 with at least 5 hours classified as cumulus and no near-overcast conditions with a cloud cover larger than 95%, which results in a total of 20 days. These days were simulated with MicroHH to select the days where the simulated cloud cover visually matches the observed cloud cover, which results in a selection of 12 days. From these 12 days, the last hours (17-21 UTC) of 4 July 2016 were excluded from further analysis, as the clouds are not surface driven during these hours.

2.2 Model simulations

2.2.1 General setup

We used MicroHH (van Heerwaarden et al., 2017) to perform realistic LESs. Here we only describe the model domain and the settings that regard the radiative transfer, as it is practically unfeasible to describe all model settings of these LESs. Our complete model setup can be found in the supplementary material.

For the clear sky days, we used a domain size of 12.8 x 12.8 x 4 km^3, with a horizontal resolution of 50 m and a vertical resolution of 25 m and the simulations run from 6 - 18 UTC. For each day, we performed two simulations: one with and one without aerosols. Our simulations of the cumulus days have the same horizontal and vertical resolution as the clear-sky days, but a larger domain size of 25.6 x 25.6 x 6.4 km^3 and they run longer, from from 3 - 21 UTC. In all simulations, we used an interactive land-surface scheme, similar to HTESSEL (Balsamo et al., 2009), for which our land surface is a homogeneous grassland with an instantaneous response (in other words, the skin heat capacity is zero). Initial and boundary conditions were derived from ERA5 using $(LS)^2D$ (van Stratum et al., 2023).

In all simulations radiation is calculated every minute using RTE+RRTMGP (Pincus et al., 2019) and for the 3D radiation, we used the ray tracer of Veerman et al. (2022). For the impact of gases on radiation, we used time and height dependent

https://doi.org/10.5194/egusphere-2024-1519
Preprint. Discussion started: 24 May 2024

water vapor from our simulations, ozone from ERA5 (Hersbach et al., 2020), and carbon monoxide and methane from the CAMS global greenhouse gas reanalysis (Inness et al., 2019a). The other gases that influence radiation are assumed constant and were taken from RFMIP (Pincus et al., 2016). As our domain top is at 6.4 km, MicroHH accounts for the impact of gases and aerosols on radiation above our domain top, by calculating radiation for one column that extends until the top of the atmosphere. This background column consists of time and height dependent ERA5 data (temperature, pressure, water vapor, and ozone at the native ERA5 model levels), combined with time and height dependent carbon monoxide and methane from CAMS, and constant gases from RFMIP.

For each cumulus day, we performed two simulations: one with coupled 1D radiation and one with coupled 3D radiation. In these coupled simulations, the results of the radiative transfer calculations impact the surface and atmosphere. Here (and in the remainder of this work), *1D radiation* is short for 1D radiative transfer which means that we used the two-stream approach and *3D radiation* is short for 3D radiative transfer which means that we used the ray tracer. We performed 3 simulations of each cumulus day/coupled radiation method with a different random seed for the initial random perturbations, to estimate statistical convergence of our simulation results. Our plots show the average result of the 3 simulations, unless indicated otherwise.

2.2.2 Link between radiation and clouds

To understand the differences in clouds between the simulations with coupled 1D and 3D radiation, we investigated the link between radiation and clouds. Based on previous research (Veerman et al., 2020; Jakub and Mayer, 2017; Veerman et al., 2022), we hypothesized that changes in the distribution of surface radiation alter the surface energy balance, which modifies the updrafts that link the surface to the clouds, resulting in a change in clouds. These changes occur because with 3D radiation the cloud shadows are displaced, thus cloud shadows are not directly below the clouds and cloud enhancements can occur. In the shadows, the fluxes are reduced, and in the cloud enhancements the fluxes are increased. These differences in surface fluxes determine where updrafts are likely to form, and therefore where clouds grow.

Our hypothesis also shows the complexity of the problem. Changes in clouds will affect the surface radiation, which makes it complex to determine what is the cause and what is the consequence, and it is hard to prove any causality. However, we can investigate if our simulations support our hypothesis by looking at the correlations between the cloud shadow displacement and the changes in clouds. Since the changes in liquid water path, cloud cover and cloud depth are related, we only examined the relative difference in liquid water path, which is the difference in liquid water path between the simulations with 3D and 1D radiation relative to the liquid water path in the simulation with 1D radiation. We described the cloud shadow displacement relative to the cloud with three factors: 1. The distance between the cloud and its shadow (derived from the domain-averaged cloud base height and solar zenith angle); 2. The angle between the sun and the wind (derived from the wind direction at 500 m and the solar azimuth angle); 3. The wind speed at 500 m.

To test our hypothesis, we focused on the times between cloud onset and the time with the maximum domain-averaged liquid water path. After a similar cloud onset, the clouds in simulations with 1D and 3D radiation can start to differ as 3D radiative effects start to play a role, so we only investigated times after cloud onset. Later on, dissipation of the clouds starts to play an important role in the development of the cloud field. As we expect the clouds in the simulations with 3D radiation to be thicker

https://doi.org/10.5194/egusphere-2024-1519
Preprint. Discussion started: 24 May 2024

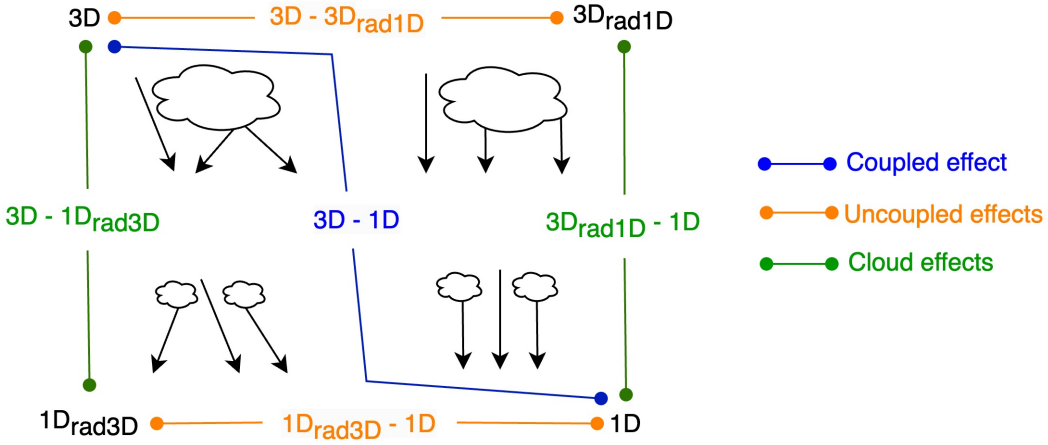

Figure 1. Schematic overview of the simulations with coupled and uncoupled radiation. The simulation with coupled 3D radiation is in the top left (3D), the simulation with coupled 1D radiation is in the bottom right (1D). The top right is the uncoupled 1D radiation of our simulation with coupled 3D radiation, the bottom left is the uncoupled 3D radiation of our simulation with coupled 1D radiation. The blue line indicates the coupled effect, the orange lines the two different uncoupled effects, and the green lines the two different cloud effects.

and larger (Veerman et al., 2020, 2022), they will dissipate slower. We argue that this is mainly important after the maximum domain-averaged liquid water path is reached, and therefore we only investigated times before this maximum.

2.2.3 Uncoupled radiation computations

To understand the differences in radiation between the simulations with coupled 1D and 3D radiation, we performed additional uncoupled radiation computations, which means that the results of the radiative transfer calculations do not impact the surface and atmosphere. Our setup is shown schematically in Fig. 1, where the simulations with coupled 3D radiation and coupled 1D radiation as described in Sect. 2.2.1 are located in the top left and bottom right of the schematic. The impact of coupled 3D radiation, hereafter referred to as the coupled effect, is the difference between the two, so 3D – 1D, which is indicated with the blue line in Fig.1.

We calculated two types of uncoupled radiation: uncoupled 3D radiation and uncoupled 1D radiation. For the uncoupled 3D radiation, indicated in the bottom left of Fig. 1 ($1D_{rad3D}$), we took the cloud fields from the simulations with coupled 1D radiation and perform offline 3D radiation computations. This approach is similar to what has been done in previous studies (e.g., Gristey et al., 2020a, b). For the uncoupled 1D radiation ($3D_{rad1D}$), indicated in the top right of Fig. 1, we took the cloud fields from the simulations with coupled 3D radiation and perform offline 1D radiation computations.

We used these additional calculations to split the difference between 3D and 1D in two parts. The first part is the uncoupled effect, which is indicated with the orange lines in Fig. 1. This is the difference in radiation that occurs when the radiative transfer method differs, but the clouds are the same. The uncoupled effect using uncoupled 3D radiation was studied before,

https://doi.org/10.5194/egusphere-2024-1519
Preprint. Discussion started: 24 May 2024

e.g. by Gristey et al. (2020a). The second part is the cloud effect, which is indicated with the green lines in Fig. 1. This is the difference in radiation that occurs when the clouds are different, but the radiative transfer method is the same. We are aware that physically the two effects can not be seen separate from each other, but purely from a mathematical point of view, the two effects add up to the coupled effect, and the separate effects are easier to understand, as we will show in Sect. 4.2. We obtained both the uncoupled effect and cloud effect in two ways, using either $3D_{rad1D}$ or using $1D_{rad3D}$, as is visible in Fig. 1. In Sect. 4.2, we will show how the uncoupled effect and cloud effect differ between the two ways of splitting.

2.2.4 Aerosols

Previous studies have shown the importance of aerosols when simulating radiation realistically (Schmidt et al., 2009; Gristey et al., 2022; Tijhuis et al., 2023). Therefore, we created the option in MicroHH to use aerosol data from the CAMS global reanalysis to include the direct effect of aerosols in our simulations. We chose to use the aerosol data from CAMS (Inness et al., 2019a) for this purpose, as it is also used e.g. in IFS (Bozzo et al., 2017) and to study aerosol-radiation interactions in Witthuhn et al. (2021). The dataset includes information for 11 different aerosol types, namely organic matter (hydrophilic and hydrophobic), black carbon (hydrophilic and hydrophobic), sea salt (in 3 size ranges), dust (in 3 size ranges), and sulphates.

From the CAMS dataset, we used the aerosol mass mixing ratios at the CAMS model levels, which we obtained with the same workflow as we used to include the ERA5 meteorology (van Stratum et al., 2023). Thus, we downloaded the vertical profiles based on a give location (lat/lon), after which we interpolated the data to both the LES vertical levels and the ERA5 model levels, the latter being necessary for the calculations of the radiation above the domain as described in Sect. 2.2.1. In our simulations, the aerosol mass mixing ratios were linearly interpolated in time and then converted to optical properties using a pre-calculated lookup table with aerosol optical properties (Bozzo et al., 2020). The optical properties in this table are given per class of 10% relative humidity. We used these optical properties directly, without interpolation between the classes. For our model domain, we combined one profile of aerosol mass mixing ratios with the 3D relative humidity in our simulation, resulting in aerosol optical properties that also varied in the horizontal. For our background profile, we used the relative humidity from ERA5. Finally, the aerosol optical properties were combined with the optical properties of the gases and the clouds, to form the total set of optical properties that was used for the radiation calculations.

3 Validation

We compare our simulations with observations from the Royal Netherlands Meteorological Institute (KNMI) site at the Ruisdael Observatory in Cabauw, the Netherlands. First, we validate our implementation of the aerosols for the clear sky days using the observations from the BSRN station (Mol et al., 2023). Next, we validate the cumulus cases, for which we use the temperature, specific humidity, and wind measurements from the measurement tower (KNMI Data Services, 2024b) and the cloud cover measurements of the Nubiscope, which is a scanning infrared radiometer (KNMI Data Services, 2024a).

For the clear sky days, we compare the global, direct, and diffuse radiation of our simulations with the observations in Fig. 2. In the simulations without aerosols (top row), we notice that the simulated direct radiation is too high compared to the

https://doi.org/10.5194/egusphere-2024-1519
Preprint. Discussion started: 24 May 2024

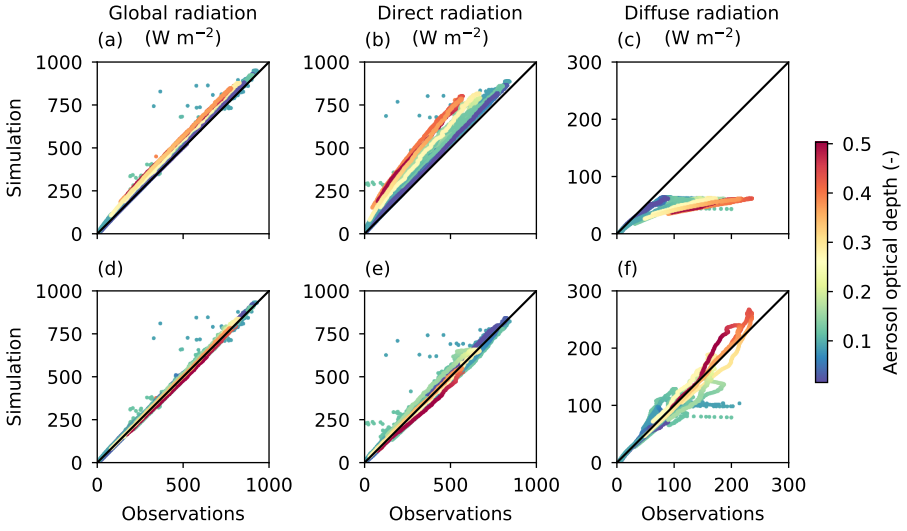

Figure 2. Comparison of simulated and observed surface solar radiation on clear sky days. The top row shows simulations without aerosols, the bottom row simulations with aerosols.

observations and the diffuse radiation is too low, because the scattering effect of the aerosols is missing. Also, we see that the global radiation is slightly overestimated in the simulations compared to the observations, as the aerosols also absorb some radiation and increase the scattering back upwards. In the simulations with aerosols (bottom row), the direct, diffuse, and global radiation are well in line with the observations. This demonstrates that we can use the aerosol data from CAMS to remove a mean bias in the global, direct, and diffuse radiation.

For the cumulus days, we compare the observed and simulated cloud cover in Fig. 3. The selected days cover a range of cumulus cloud conditions with the maximum simulated cloud cover between 0.2 and 0.75. Validation plots of the temperature, specific humidity, and wind speed are included in the Appendix. In general, the simulations are well in line with the observations, which shows that our simulations realistically represent these days. Some differences between the observed and simulated cloud cover are expected, since we are comparing our domain-averaged cloud cover with the observations of a scanning instrument. However, we miss part of the variability in cloud cover, which is likely because of the limited domain size and double-periodic boundaries of our simulations, which prohibit the formation of meso-scale structures (e.g., Schalkwijk et al., 2015; Heinze et al., 2017; Schemann et al., 2020; van Stratum et al., 2023).

4 Results

We first compare the clouds in the simulations with 1D and 3D radiation in Sect. 4.1, after which we investigate the differences in domain-averaged surface radiation in Sect. 4.2.

https://doi.org/10.5194/egusphere-2024-1519
Preprint. Discussion started: 24 May 2024

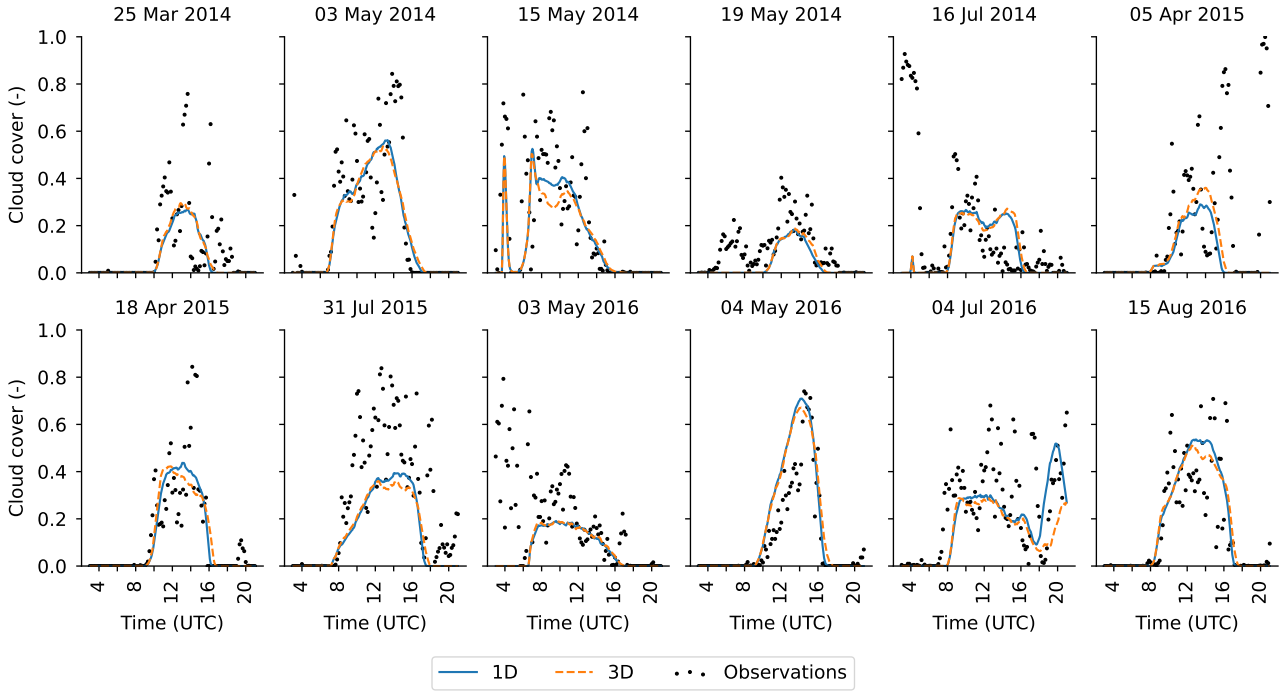

Figure 3. Time series of simulated and observed cloud cover on the 12 selected cumulus cloud days.

4.1 Changes in clouds

Figures 4a, b, and c show the cloud cover, cloud depth, and liquid water path of the simulations with 1D and 3D radiation. The cloud cover is generally similar in the simulations with 1D and 3D radiation, but the cloud depth (defined as the distance between the lowest and highest model level with any liquid water) and liquid water path clearly differ. Simulation with 3D radiation have deeper clouds and a higher liquid water path than simulations with 1D radiation. The higher liquid water path is partly because of the deeper clouds, although the additional layers with liquid water in the simulations with 3D radiation contain relatively little liquid water, so the difference in liquid water path is mainly because of higher liquid water concentrations.

Furthermore, we investigate the characteristic length scale of the specific humidity spectrum averaged over the cloud layer, as defined in Veerman et al. (2020) (and references therein), because the spectrum of specific humidity can give an indication of the important cloud sizes (Veerman et al., 2022). This length scale is shown in Fig. 4d, where the development of the length scale during the day can be seen from the colors that indicate the normalized time between the first and last time step with any liquid water. The characteristic length scale increases during the day in both simulations, as the clouds develop during the day. However, in the simulations with 3D radiation, the characteristic length scale increases more than in simulations with 1D radiation. We find a similar pattern for the characteristic length scale of the vertical velocity spectrum in the boundary layer (between 450 and 550 m, not shown), with larger length scales in the simulations with coupled 3D radiation. These increases

https://doi.org/10.5194/egusphere-2024-1519
Preprint. Discussion started: 24 May 2024

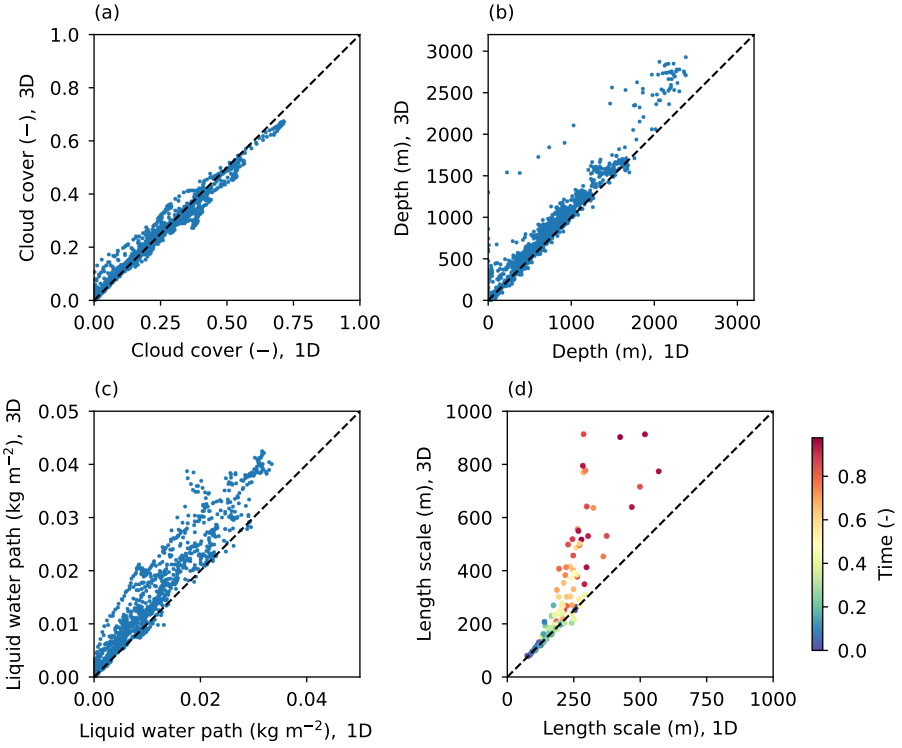

Figure 4. Comparison of the domain-averaged cloud characteristics of the simulations with 1D radiation and 3D radiation. (a) cloud cover, (b) cloud depth, (c) liquid water path, (d) characteristic length scale of specific humidity in the cloud layer. The length scales are determined from one simulation per radiation type instead of being the average of three simulations. The colors in (d) indicate the normalized time between the first and last timestep with any liquid water.

in the length scales of vertical velocity and specific humidity show that the turbulent structures become larger, which results in larger clouds.

Our findings generalize the results of Veerman et al. (2020), who found larger and thicker clouds, and Veerman et al. (2022), who found an increase in liquid water path, wider clouds, and a similar cloud cover. Thus, simulations with 3D radiation develop deeper and wider clouds with a higher liquid water path but similar cloud cover as simulations with 1D radiation.

As described in Sect. 2, the two-way feedback between clouds and surface radiation obscures the origin of deeper and wider clouds under similar cloud cover, but the variation among our cases can shed some light on which changes in the surface radiation matter for cloud development. To this end, we focus on the correlation between the cloud shadow displacement and the changes in liquid water path. We find the highest correlation between the relative difference in liquid water path and the wind-sun angle (r = 0.55). If the wind-sun angle is small, a cloud moves in the direction of its own shadow, where the surface fluxes are reduced. This suppresses the formation of updrafts, and is therefore disadvantageous for the growth of the cloud. Hence, the clouds in the 3D simulations cannot grow bigger than in the simulations with 1D radiation and the relative

https://doi.org/10.5194/egusphere-2024-1519
Preprint. Discussion started: 24 May 2024

difference in liquid water path is small. In contrast, if the wind-sun angle is large, the cloud does not travel over its own shadow, but instead over a sunlit area that potentially receives additional radiation through cloud enhancements. The updrafts likely form in these sunlit areas and the cloud will be enforced by these updrafts, causing the cloud to live longer and therefore potentially grow more than in a simulation with 1D radiation. Hence, the relative difference in liquid water path is large. Therefore, the correlation between the wind-sun angle and the relative difference in liquid water path supports the hypothesis that the 3D effects propagate via the surface.

The other investigated factors, wind speed and displacement distance, are also positively correlated with the relative difference in liquid water path, although the correlations are weaker (r = 0.33 and r = 0.27, respectively). As our three factors are independent of each other, we perform a multilinear regression that combines these three factors. This combination has a slightly improved correlation compared to the wind-sun-angle alone (r = 0.6). This increased correlation shows that the wind speed and displacement distance also play a role, but their impact is not as clear as for the wind-sun angle. Furthermore, we note that the three factors combined do not fully explain the relative difference in liquid water path. This highlights the complexity of the problem, where clouds can also be influenced by the shadows of other clouds and by other factors that control cloud formation, such as the stability of the layer above the clouds or the soil moisture content.

4.2 Changes in radiation

In this section, we investigate the differences in domain-averaged surface radiation. We first describe the coupled effect, so radiation from the simulations with 3D radiation minus radiation from the simulations with 1D radiation. Then, we describe and explain the uncoupled effect and cloud effect. We end this section by explaining the coupled effect using the uncoupled effect and cloud effect. For each effect, we show time series of the effect for one arbitrarily selected example day (3 May 2014, Fig. 5) and box plots including all days (Fig. 6).

Figure 5a shows the mean differences in radiation between the simulations with 3D radiation and the simulations with 1D radiation on one day. On this day, increases and decreases in global, direct, and diffuse radiation all occur when using coupled 3D radiation instead of coupled 1D radiation. Also shown in the figure is the spread between the three simulation realizations of the selected day. The spreading illustrates that the trends and sign are the same across the repeated simulations, although the exact magnitude of the effects differs.

The mean coupled effect for all days is summarized in the box plots in Fig. 6a. On average, the direct radiation decreases in the simulations with 3D radiation compared to the simulations with 1D radiation, the diffuse radiation increases, and the global radiation stays approximately the same. However, individual moments can deviate strongly from this general pattern, for example the difference in global radiation can be more than +/- 25 W m^{-2} instantaneously.

To understand the coupled effect better, we separate it in the uncoupled effect and the cloud effect, which are shown for one day in Fig. 5b and c. As explained in Sect. 2, we can split the coupled effect using the uncoupled 1D radiation (the lines in Fig. 5) or using the uncoupled 3D radiation (the dots in Fig. 5). Comparing the two splitting methods shows that the exact magnitude of the effects depends on the splitting method, which is not surprising for the day in Fig. 5 given the large difference in domain-averaged liquid water path (up to 0.012 kg m^{-2}) between the simulation with 1D and 3D radiation. However, the

https://doi.org/10.5194/egusphere-2024-1519
Preprint. Discussion started: 24 May 2024

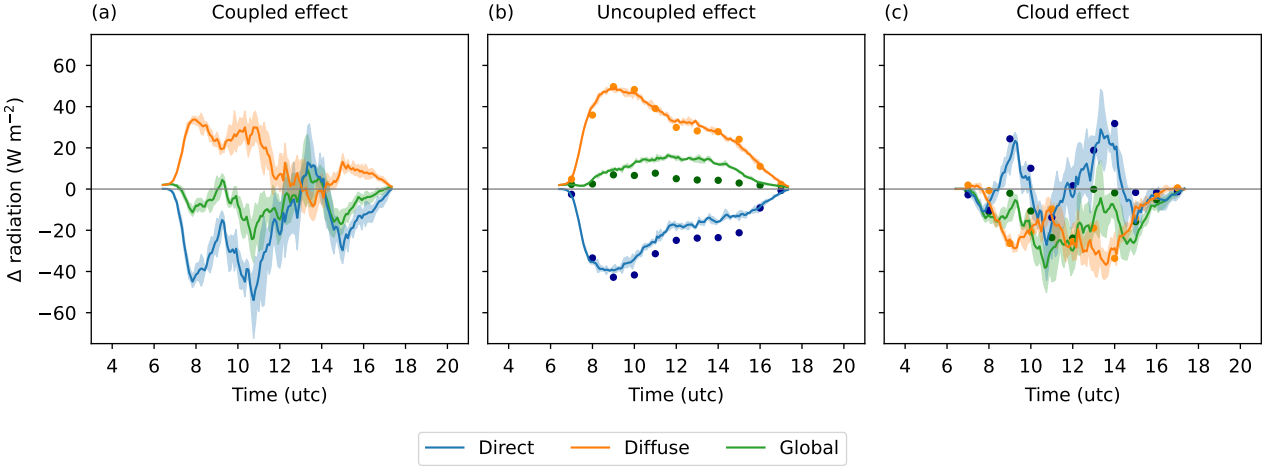

Figure 5. Time series of the coupled effect (a), uncoupled effect (b), and cloud effect (c) on 3 May 2014. In (b) and (c), the dots show the effect when using uncoupled 3D radiation ($1D_{rad3D}$) and the lines show the effect when using uncoupled 1D radiation ($3D_{rad1D}$). The shading shows the range of the differences between the three repetitions of each simulation.

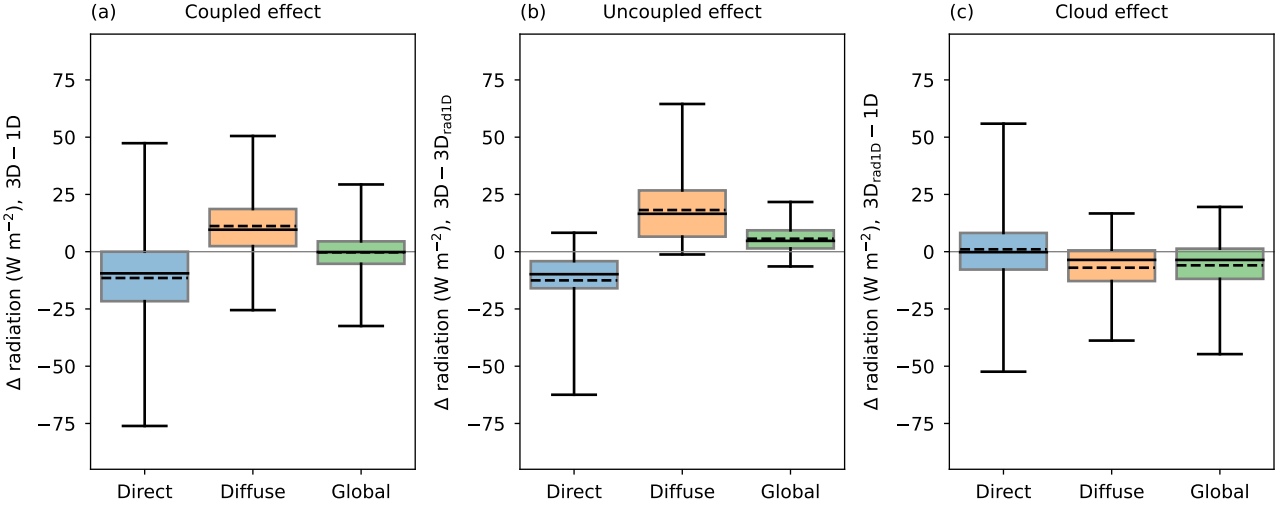

Figure 6. Box plot of the coupled effect (a), uncoupled effect (b), and cloud effect (c) in direct, diffuse and global radiation. The whiskers range from the minimum to the maximum difference, the full line indicates the median, and the dashed line shows the mean.

https://doi.org/10.5194/egusphere-2024-1519
Preprint. Discussion started: 24 May 2024

trends and sign of the effects are the same between the splitting methods, thus we can use either method to explain them. We opt for the splitting using uncoupled 1D radiation, as this splitting method has the advantage that we compare two versions of 1D radiation for the cloud effect, which is the simplest to understand, and the uncoupled 1D radiation is available at higher frequency than the uncoupled 3D radiation (see Fig. 5).

4.2.1 The uncoupled effect

First, we look at the uncoupled effect, which is the difference between 1D and 3D radiation for the same clouds. Figure 5b shows the uncoupled effect for one day, but we find a similar pattern for the other 11 days (not shown). Figure 6b shows box plots of the uncoupled effect using uncoupled 1D radiation for all cases together. Both plots show that for a given cloud field the direct radiation decreases with 3D radiation compared to 1D radiation, and both the diffuse radiation and global radiation increase. These changes are in line with the results of Gristey et al. (2020a), where they also explain how these results are the combination of side-escape, side-illumination, and entrapment. In short, diffuse radiation increases because of the side escape and entrapment, whereas direct radiation decreases because of side illumination. Gristey et al. (2020a) also found that the difference in direct radiation can sometimes be positive. We see this as well for a short moment on one day. In our case, this is because the clouds are tilted along the angle of the incoming sunlight. In summary, for our cases (and also for the ones in Gristey et al. (2020a)), the uncoupled effect is an increase in diffuse radiation and a decrease in direct radiation, which combined results in a net increase in global radiation.

4.2.2 The cloud effect

Next, we look at the cloud effect, which can be seen as a difference in radiation caused by a change in clouds. Since we use the uncoupled 1D radiation, we are looking at the difference in 1D radiation between two simulations with different clouds (namely the simulation with coupled 3D radiation and the simulation with coupled 1D radiation). This difference is indicated with the right green line in Fig. 1 ($3D_{rad1D}$ - 1D). The lines in Fig. 5c show this cloud effect for one day, and Fig. 6c shows box plots of this cloud effect for all cases together.

For the largest part of the day in Fig. 5, the direct radiation is higher when calculating uncoupled 1D radiation of a simulation with coupled 3D radiation ($3D_{rad1D}$) compared to the simulations with coupled 1D radiation. However, for a short period, there is a decrease. Conversely, both the diffuse and global radiation decrease. Looking at all 12 days, there is no clear daily pattern (not shown). Figure 6c reveals that increases and decreases in direct radiation occur roughly equally much, but typically both the diffuse and global radiation decrease. Thus, in contrast to the uncoupled effect, the cloud effect is a net decrease in global radiation.

The changes in direct and diffuse radiation, and therefore the net decrease in global radiation, are correlated with the changes in clouds. In general, the direct radiation at the surface is minimal in cloud shadows and high in clear sky areas. Consequently, a change in direct radiation is mainly caused by differences in shadowed area. As we are comparing 1D radiation of different cloud fields, a difference in shadowed area means a difference in cloud cover. Figure 7a confirms that the differences in direct

https://doi.org/10.5194/egusphere-2024-1519
Preprint. Discussion started: 24 May 2024

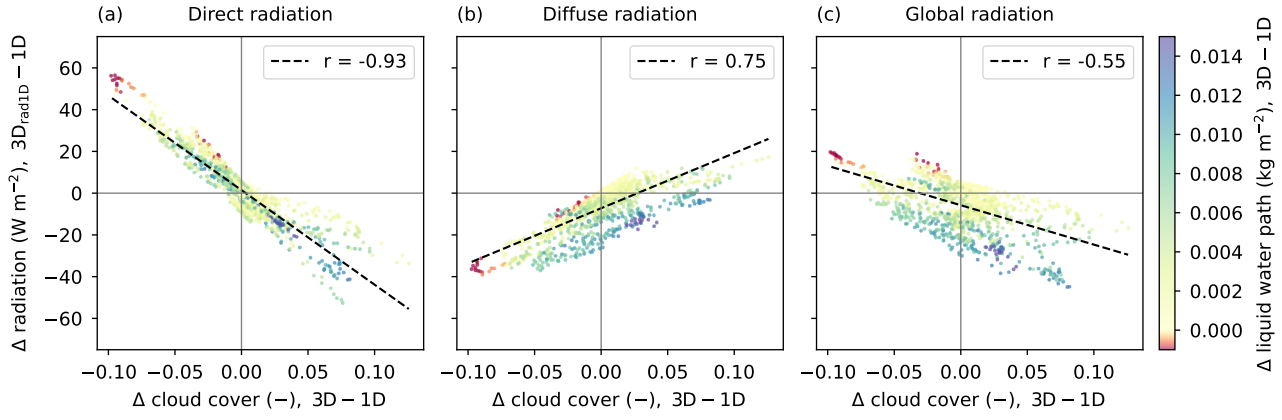

Figure 7. The cloud effect as a function of the difference in cloud cover. (a) Direct radiation, (b) diffuse radiation, and (c) global radiation. The colors indicate the difference in liquid water path. The black dotted line shows the linear trend with the correlation coefficient (r).

radiation are strongly anti-correlated with the differences in the cloud cover, and that there is no difference in direct radiation when the cloud cover is the same in the simulations with 3D and 1D radiation.

The opposite reasoning holds for the differences in diffuse radiation, which is shown in Fig. 7b. The diffuse radiation increases when the cloud cover is higher in the simulation with 3D radiation compared to the simulation with 1D radiation. However, the differences in diffuse radiation are not only caused by differences in cloud cover, but also by differences in liquid water path, as can be seen from the colors in Fig. 7b. When the liquid water path is higher, there is less diffuse radiation at the surface because there is more absorption and more scattering back upwards.

Combining the cloud effect on direct and diffuse radiation results in the cloud effect in global radiation shown in Fig. 7c. This effect is not as strongly correlated with the difference in cloud cover, because the direct and diffuse effect partly cancel each other out. Apart from more radiation being scattered downwards, an increased cloud cover also increases upward scattering and absorption, which reduces the global radiation at the surface. Therefore, the difference in global radiation is negatively correlated with the difference in cloud cover. Similar to the difference in diffuse radiation, the difference in global radiation is also related to the difference in liquid water path, as a larger increase in liquid water path corresponds to a larger decrease in global radiation.

4.2.3 The coupled effect

The uncoupled effect and the cloud effect together give the coupled effect from the beginning of this section: a decrease in direct radiation, an increase in diffuse radiation, and no change in global radiation. We can now explain this coupled effect, using the uncoupled effect and cloud effect.

Figure 8 shows the correlation between the changes in global radiation and the changes in clouds. Similar to what we see for the cloud effect, the changes in global radiation and cloud cover are negatively correlated (Fig. 8a). The trend line shows

https://doi.org/10.5194/egusphere-2024-1519
Preprint. Discussion started: 24 May 2024

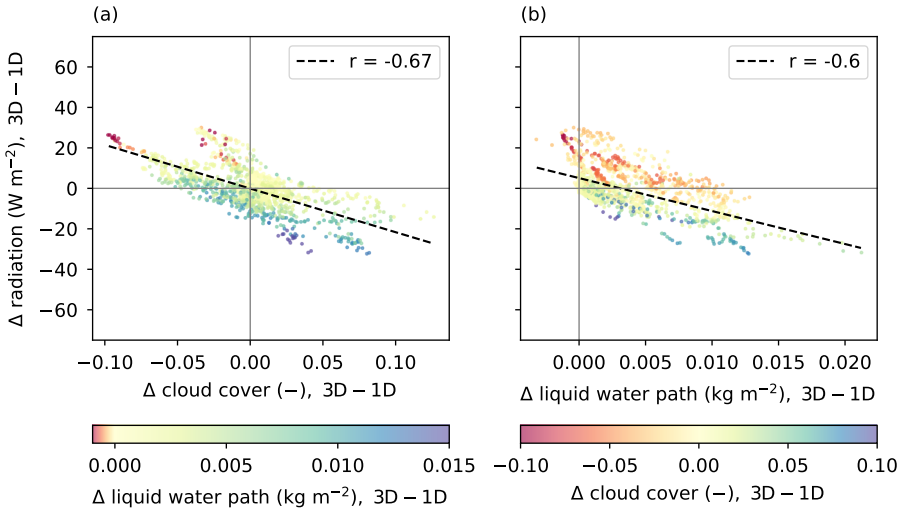

Figure 8. The coupled effect in global radiation as a function of the difference in cloud cover (a) and liquid water path (b). The colors indicate the difference in liquid water path (a) or cloud cover (b). The black dotted line shows the linear trend with the correlation coefficient (r).

that there is no difference in global radiation when there is no difference in cloud cover, which is in line with what we find on average for our 12 days. Comparing Fig. 8a and Fig. 7c reveals that the coupled effect in global radiation is largely comparable to the cloud effect in global radiation. The strong similarity between these figures emphasizes how important the changes in clouds are for the coupled effect.

We can also recognise the uncoupled effect in the coupled effect from the correlation between the differences in global radiation and the differences in liquid water path (Fig. 8b). When the difference in liquid water path (and cloud cover) is close to zero, the global radiation is higher in simulations with coupled 3D radiation. Thus, when the clouds are the same, 3D radiation gives less global radiation, which is also what we find as the uncoupled effect. Following a similar reasoning, Figure 8b shows that the global radiation is the same in the simulations with 1D and 3D radiation, when the simulation with 3D radiation has an increased liquid water path, which is exactly what we find on average for our 12 days.

5 Conclusions and outlook

We studied the impact of 3D radiation on cumulus clouds and the domain-averaged surface radiation, by comparing coupled 1D and coupled 3D radiation for 12 cumulus cases. We found that coupled 3D radiation increases cloud liquid water path and cloud size (both in the horizontal and in the vertical), but without affecting the cloud cover. The domain-averaged surface global radiation is also on average unchanged because of two opposing effects. On the one hand, uncoupled 3D radiation causes a decrease in direct radiation by side illumination and an increase in diffuse radiation by side escape and entrapment, resulting in a net increase in global radiation. On the other hand, an increase in liquid water path of the clouds causes a decrease in global radiation.

https://doi.org/10.5194/egusphere-2024-1519
Preprint. Discussion started: 24 May 2024

Our results show that the necessity for coupled 3D radiation depends on your goals. For example, the increased cloud size and liquid water path might feed back to rain formation, which is relevant for weather prediction applications. Furthermore, the shift in the partitioning between direct and diffuse radiation can influence photosynthesis and energy production by solar panels. In addition, the current results might be used in future research to validate parameterizations of 3D effects when these parameterizations are coupled to simulations.

Future work could tackle the limitations of the current work, to generalize our results further. For example, the coupled ray tracer could be extended to the longwave spectral range, as previous research has shown that 3D longwave radiation also influences the clouds (see e.g. Schäfer et al. (2016); Klinger et al. (2017)). In addition, our clouds are currently bound by the limited domain size and periodic lateral boundaries, which future research could improve on by using open boundaries. Moreover, it is not trivial to determine from our current simulations which factors determine the magnitude of the differences between simulations with 1D and 3D radiation. To this end, a more idealistic setup, in which one factor is changed at a time, might yield further insights. Lastly, the current work focuses on cumulus clouds over grassland in the mid-latitudes. The impact of coupled 3D radiation is potentially different for other cloud types, where the coupling with the surface is less important. Moreover, the impact of coupled 3D radiation is potentially different for other locations with different surface properties or different latitudes with different solar zenith angles.

Nonetheless, we believe that our 12 cases cover the most common conditions with cumulus over grassland in the mid-latitudes and that our results are representative for those conditions. Hence, we conclude that, coupled 3D radiation deepens cumulus clouds without changing the mean surface solar irradiance.

Code and data availability. The observations of temperature, humidity, wind and cloudcover at the measurement station in Cabauw are openly available from the KNMI Data Platform (KNMI Data Services, 2024a, b). The observations of radiation and the additional data used to select the cases are openly available from Knap and Mol (2022) and Mol et al. (2022). The CAMS global reanalysis data is openly available from Inness et al. (2019b) and Inness et al. (2019c). The model simulations are performed with MicroHH (van Heerwaarden et al., 2017) version 2.0.0_RC1, which is openly available at https://github.com/microhh/microhh/releases/tag/2.0.0_RC1, coupled to ERA5 using $(LS)^2D$ (van Stratum et al., 2023), which is openly available at https://github.com/LS2D/LS2D and https://pypi.org/project/ls2d/. The complete model set-up of our simulations as well as scripts to analyse the simulation results can be found at https://doi.org/10.5281/zenodo.11234717

Appendix A

Figure A1 shows the observed and simulated temperature, specific humidity and wind speed.

Author contributions. MT performed the simulations and analysis and wrote the manuscript in close collaboration with BvS and CvH.

https://doi.org/10.5194/egusphere-2024-1519
Preprint. Discussion started: 24 May 2024

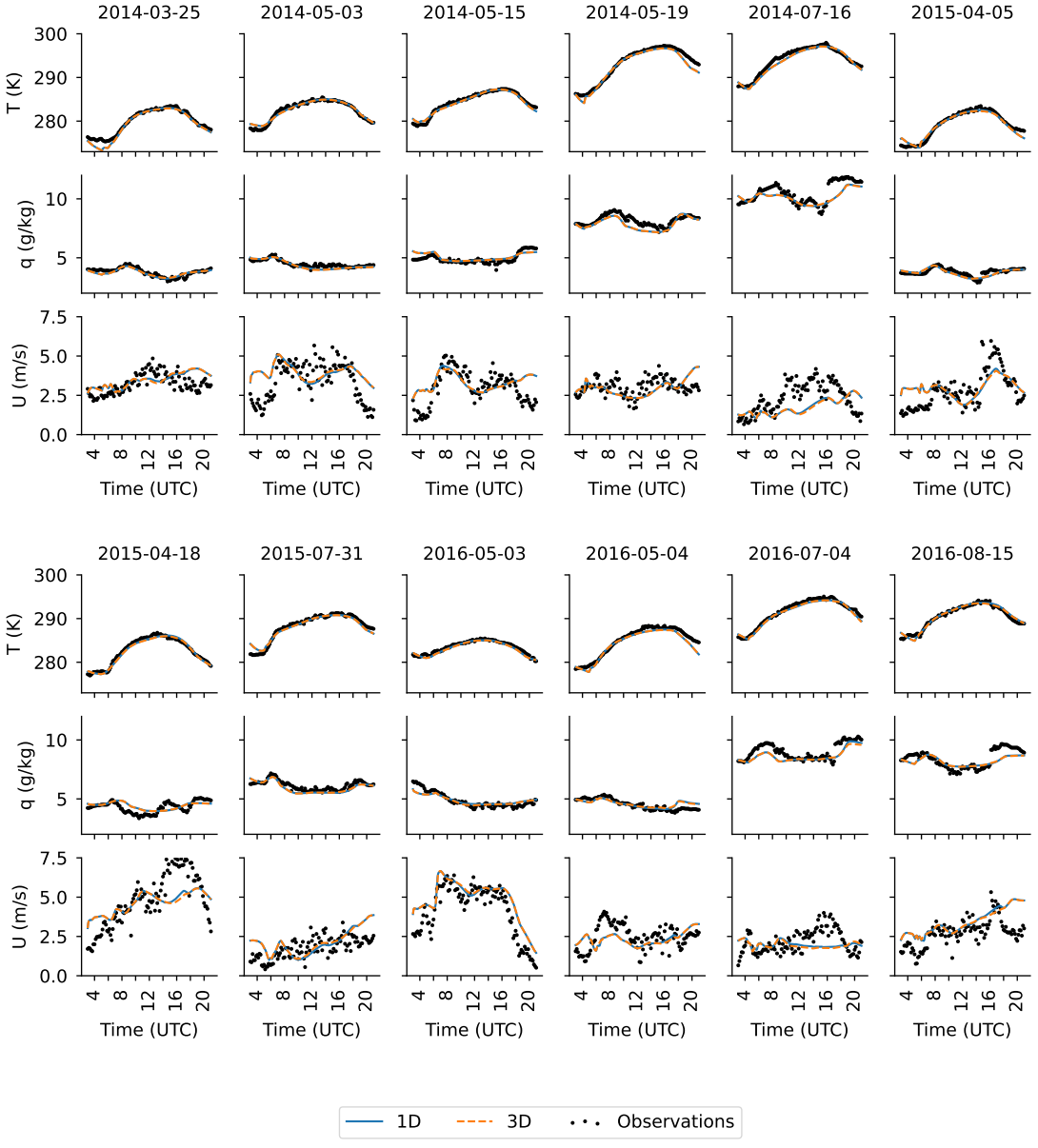

Figure A1. Time series of simulated and observed temperature (first and fourth row), specific humidity (second and fifth row), and wind speed (third and sixth row) on the 12 selected cumulus cloud days. Observations are at 10 m height and values from the simulation are taken at 12.5 m height.

https://doi.org/10.5194/egusphere-2024-1519
Preprint. Discussion started: 24 May 2024

Competing interests. The authors declare that they have no conflict of interest.

Acknowledgements. We acknowledge funding from the Wageningen Institute for Environment and Climate Research (WIMEK) and the Shedding Light On Cloud Shadows project funded by the Dutch Research Council (NWO) (grant: VI.Vidi.192.068). The simulations are carried out on the Dutch national e-infrastructure with the support of SURF Cooperative (project numbers NWO-2021.036 and NWO-2023.003).

https://doi.org/10.5194/egusphere-2024-1519
Preprint. Discussion started: 24 May 2024

References

Balsamo, G., Beljaars, A., Scipal, K., Viterbo, P., van den Hurk, B., Hirschi, M., and Betts, A. K.: A revised hydrology for the ECMWF model: Verification from field site to terrestrial water storage and impact in the Integrated Forecast System, Journal of hydrometeorology, 10, 623–643, 2009.

Bozzo, A., Remy, S., Benedetti, A., Flemming, J., Bechtold, P., Rodwell, M. J., and Morcrette, J.: Implementation of a CAMS-based aerosol climatology in the IFS, vol. 801, European Centre for Medium-Range Weather Forecasts Reading, UK, 2017.

Bozzo, A., Benedetti, A., Flemming, J., Kipling, Z., and Rémy, S.: An aerosol climatology for global models based on the tropospheric aerosol scheme in the Integrated Forecasting System of ECMWF, Geoscientific Model Development, 13, 1007–1034, https://doi.org/10.5194/gmd-13-1007-2020, 2020.

Cahalan, R. F., Oreopoulos, L., Marshak, A., Evans, K. F., Davis, A. B., Pincus, R., Yetzer, K. H., Mayer, B., Davies, R., Ackerman, T. P., Barker, H. W., Clothiaux, E. E., Ellingson, R. G., Garay, M. J., Kassianov, E., Kinne, S., Macke, A., O'hirok, W., Partain, P. T., Prigarin, S. M., Rublev, A. N., Stephens, G. L., Szczap, F., Takara, E. E., Várnai, T., Wen, G., and Zhuravleva, T. B.: THE I3RC: Bringing Together the Most Advanced Radiative Transfer Tools for Cloudy Atmospheres, Bulletin of the American Meteorological Society, 86, 1275 – 1294, https://doi.org/10.1175/BAMS-86-9-1275, 2005.

Gristey, J. J., Feingold, G., Glenn, I. B., Schmidt, K. S., and Chen, H.: Surface Solar Irradiance in Continental Shallow Cumulus Fields: Observations and Large-Eddy Simulation, Journal of the Atmospheric Sciences, 77, 1065–1080, https://doi.org/https://doi.org/10.1175/JAS-D-19-0261.1, 2020a.

Gristey, J. J., Feingold, G., Glenn, I. B., Schmidt, K. S., and Chen, H.: On the Relationship Between Shallow Cumulus Cloud Field Properties and Surface Solar Irradiance, Geophysical Research Letters, 47, https://doi.org/10.1029/2020GL090152, 2020b.

Gristey, J. J., Feingold, G., Schmidt, K. S., and Chen, H.: Influence of Aerosol Embedded in Shallow Cumulus Cloud Fields on the Surface Solar Irradiance, Journal of Geophysical Research: Atmospheres, 127, https://doi.org/https://doi.org/10.1029/2022JD036822, 2022.

Gronemeier, T., Kanani-Sühring, F., and Raasch, S.: Do shallow cumulus clouds have the potential to trigger secondary circulations via shading?, Boundary-Layer Meteorology, 162, 143–169, 2017.

Heinze, R., Dipankar, A., Henken, C. C., Moseley, C., Sourdeval, O., Trömel, S., Xie, X., Adamidis, P., Ament, F., Baars, H., Barthlott, C., Behrendt, A., Blahak, U., Bley, S., Brdar, S., Brueck, M., Crewell, S., Deneke, H., Di Girolamo, P., Evaristo, R., Fischer, J., Frank, C., Friederichs, P., Göcke, T., Gorges, K., Hande, L., Hanke, M., Hansen, A., Hege, H.-C., Hoose, C., Jahns, T., Kalthoff, N., Klocke, D., Kneifel, S., Knippertz, P., Kuhn, A., van Laar, T., Macke, A., Maurer, V., Mayer, B., Meyer, C. I., Muppa, S. K., Neggers, R. A. J., Orlandi, E., Pantillon, F., Pospichal, B., Röber, N., Scheck, L., Seifert, A., Seifert, P., Senf, F., Siligam, P., Simmer, C., Steinke, S., Stevens, B., Wapler, K., Weniger, M., Wulfmeyer, V., Zängl, G., Zhang, D., and Quaas, J.: Large-eddy simulations over Germany using ICON: a comprehensive evaluation, Quarterly Journal of the Royal Meteorological Society, 143, 69–100, https://doi.org/https://doi.org/10.1002/qj.2947, 2017.

Hersbach, H., Bell, B., Berrisford, P., Hirahara, S., Horányi, A., Muñoz-Sabater, J., Nicolas, J., Peubey, C., Radu, R., Schepers, D., et al.: The ERA5 global reanalysis, Quarterly Journal of the Royal Meteorological Society, 146, 1999–2049, 2020.

Hogan, R. J. and Shonk, J. K. P.: Incorporating the effects of 3D radiative transfer in the presence of clouds into two-stream multilayer radiation schemes, Journal of the atmospheric sciences, 70, 708–724, 2013.

Hogan, R. J., Schäfer, S., Klinger, C., Chiu, J. C., and Mayer, B.: Representing 3-D cloud radiation effects in two-stream schemes: 2. Matrix formulation and broadband evaluation, Journal of Geophysical Research: Atmospheres, 121, 8583–8599, 2016.

https://doi.org/10.5194/egusphere-2024-1519
Preprint. Discussion started: 24 May 2024

Hogan, R. J., Fielding, M. D., Barker, H. W., Villefranque, N., and Schäfer, S. A. K.: Entrapment: An Important Mechanism to Explain the Shortwave 3D Radiative Effect of Clouds, Journal of the Atmospheric Sciences, 76, 2123–2141, https://doi.org/10.1175/JAS-D-18-0366.1, 2019.

Horn, G. L., Ouwersloot, H. G., Arellano, J. V.-G. D., and Sikma, M.: Cloud shading effects on characteristic boundary-layer length scales, Boundary-Layer Meteorology, 157, 237–263, 2015.

Inness, A., Ades, M., Agustí-Panareda, A., Barré, J., Benedictow, A., Blechschmidt, A., Dominguez, J., Engelen, R., Eskes, H., Flemming, J., Huijnen, V., Jones, L., Kipling, Z., Massart, S., Parrington, M., Peuch, V., Razinger, M., Remy, S., Schulz, M., and Suttie, M.: The CAMS reanalysis of atmospheric composition, Atmospheric Chemistry and Physics, 19, 3515–3556, https://doi.org/10.5194/acp-19-3515-2019, 2019a.

Inness, A., Ades, M., Agustí-Panareda, A., Barré, J., Benedictow, A., Blechschmidt, A., Dominguez, J., Engelen, R., Eskes, H., Flemming, J., Huijnen, V., Jones, L., Kipling, Z., Massart, S., Parrington, M., Peuch, V., Razinger, M., Remy, S., Schulz, M., and Suttie, M.: CAMS global reanalysis (EAC4), https://ads.atmosphere.copernicus.eu/cdsapp#!/dataset/cams-global-reanalysis-eac4?tab=overview, 2019b.

Inness, A., Ades, M., Agustí-Panareda, A., Barré, J., Benedictow, A., Blechschmidt, A., Dominguez, J., Engelen, R., Eskes, H., Flemming, J., Huijnen, V., Jones, L., Kipling, Z., Massart, S., Parrington, M., Peuch, V., Razinger, M., Remy, S., Schulz, M., and Suttie, M.: CAMS global greenhous gas reanalysis (EGG4), https://ads.atmosphere.copernicus.eu/cdsapp#!/dataset/cams-global-ghg-reanalysis-egg4?tab=overview, 2019c.

Jakub, F. and Mayer, B.: A three-dimensional parallel radiative transfer model for atmospheric heating rates for use in cloud resolving models—The TenStream solver, Journal of Quantitative Spectroscopy and Radiative Transfer, 163, 63–71, 2015.

Jakub, F. and Mayer, B.: The role of 1-D and 3-D radiative heating in the organization of shallow cumulus convection and the formation of cloud streets, Atmospheric Chemistry and Physics, pp. 13 317–13 327, 2017.

Kanniah, K. D., Beringer, J., North, P., and Hutley, L.: Control of atmospheric particles on diffuse radiation and terrestrial plant productivity: A review, Progress in Physical Geography, 36, 209–237, 2012.

Klinger, C., Mayer, B., Jakub, F., Zinner, T., Park, S., and Gentine, P.: Effects of 3-D thermal radiation on the development of a shallow cumulus cloud field, Atmospheric Chemistry and Physics, 17, 5477–5500, 2017.

Knap, W. and Mol, W. B.: High resolution solar irradiance variability climatology dataset part 1: direct, diffuse, and global irradiance, https://doi.org/10.5281/zenodo.7093164, 2022.

KNMI Data Services: Clouds - cloud cover retrieved from infrared measurements at 10 minute intervals at CESAR observatory, https://dataplatform.knmi.nl/dataset/cesar-nubiscope-cldcov-la1-t10-v1-0, 2024a.

KNMI Data Services: Meteo profiles - validated and gapfilled tower profiles of wind, dew point, temperature and visibility at 10 minute interval at Cabauw, https://dataplatform.knmi.nl/dataset/cesar-tower-meteo-lc1-t10-v1-0, 2024b.

Kreuwel, F., Knap, W., Visser, L., van Sark, W., Vilà-Guerau de Arellano, J., and van Heerwaarden, C.: Analysis of high frequency photovoltaic solar energy fluctuations, Solar Energy, 206, 381–389, 2020.

Lohou, F. and Patton, E. G.: Surface Energy Balance and Buoyancy Response to Shallow Cumulus Shading, Journal of the Atmospheric Sciences, 71, 665 – 682, https://doi.org/https://doi.org/10.1175/JAS-D-13-0145.1, 2014.

Mol, W. B., Knap, W. H., and van Heerwaarden, C. C.: High resolution solar irradiance variability climatology dataset part 2: classifications, supplementary data, and statistics, https://doi.org/10.5281/zenodo.7092058, 2022.

https://doi.org/10.5194/egusphere-2024-1519
Preprint. Discussion started: 24 May 2024

Mol, W. B., Knap, W. H., and van Heerwaarden, C. C.: Ten years of 1 Hz solar irradiance observations at Cabauw, the Netherlands, with cloud observations, variability classifications, and statistics, Earth System Science Data, 15, 2139–2151, https://doi.org/10.5194/essd-15-2139-2023, 2023.

Pincus, R., Forster, P. M., and Stevens, B.: The Radiative forcing model intercomparison project (RFMIP): experimental protocol for CMIP6, Geoscientific Model Development, 9, 3447–3460, 2016.

Pincus, R., Mlawer, E. J., and Delamere, J. S.: Balancing Accuracy, Efficiency, and Flexibility in Radiation Calculations for Dynamical Models, Journal of Advances in Modeling Earth Systems, 11, 3074–3089, https://doi.org/10.1029/2019MS001621, 2019.

Schäfer, S., Hogan, R. J., Klinger, C., Chiu, J. C., and Mayer, B.: Representing 3-D cloud radiation effects in two-stream schemes: 1. Longwave considerations and effective cloud edge length, Journal of Geophysical Research: Atmospheres, 121, 8567–8582, 2016.

Schalkwijk, J., Jonker, H. J. J., Siebesma, A. P., and Bosveld, F. C.: A Year-Long Large-Eddy Simulation of the Weather over Cabauw: An Overview, Monthly Weather Review, 143, 828 – 844, https://doi.org/10.1175/MWR-D-14-00293.1, 2015.

Schemann, V., Ebell, K., Pospichal, B., Neggers, R., Moseley, C., and Stevens, B.: Linking Large-Eddy Simulations to Local Cloud Observations, Journal of Advances in Modeling Earth Systems, 12, e2020MS002 209, https://doi.org/https://doi.org/10.1029/2020MS002209, 2020.

Schmidt, K. S., Feingold, G., Pilewskie, P., Jiang, H., Coddington, O., and Wendisch, M.: Irradiance in polluted cumulus fields: Measured and modeled cloud-aerosol effects, Geophysical research letters, 36, https://doi.org/10.1029/2008GL036848, 2009.

Schumann, U., Dörnbrack, A., and Mayer, B.: Cloud-Shadow Effects on the Structure of the Convective Boundary Layer, Meteorologische Zeitschrift, 11, 285–294, lIDO-Berichtsjahr=2002,, 2002.

Tijhuis, M., van Stratum, B. J. H., Veerman, M. A., and van Heerwaarden, C. C.: An Efficient Parameterization for Surface Shortwave 3D Radiative Effects in Large-Eddy Simulations of Shallow Cumulus Clouds, Journal of Advances in Modeling Earth Systems, 15, https://doi.org/10.1029/2022MS003262, 2023.

van Heerwaarden, C., van Stratum, B. J. H., Heus, T., Gibbs, J. A., Fedorovich, E., and Mellado, J. P.: MicroHH 1.0: a computational fluid dynamics code for direct numerical simulation and large-eddy simulation of atmospheric boundary layer flows, Geoscientific Model Development, 10, 3145–3165, 2017.

van Heerwaarden, C. C., Mol, W. B., Veerman, M. A., Benedict, I., Heusinkveld, B. G., Knap, W. H., Kazadzis, S., Kouremeti, N., and Fiedler, S.: Record high solar irradiance in Western Europe during first COVID-19 lockdown largely due to unusual weather, Communications Earth & Environment, 2, 37, 2021.

van Stratum, B. J. H., van Heerwaarden, C. C., and Vilà-Guerau de Arellano, J.: The Benefits and Challenges of Downscaling a Global Reanalysis With Doubly-Periodic Large-Eddy Simulations, Journal of Advances in Modeling Earth Systems, 15, https://doi.org/https://doi.org/10.1029/2023MS003750, 2023.

Veerman, M. A., Pedruzo-Bagazgoitia, X., Jakub, F., de Arellano, J., and van Heerwaarden, C. C.: Three-dimensional radiative effects by shallow cumulus clouds on dynamic heterogeneities over a vegetated surface, Journal of Advances in Modeling Earth Systems, 12, 2020.

Veerman, M. A., van Stratum, B. J., and van Heerwaarden, C. C.: A Case Study of Cumulus Convection Over Land in Cloud-Resolving Simulations With a Coupled Ray Tracer, Geophysical Research Letters, 49, https://doi.org/10.1029/2022GL100808, 2022.

Vilà-Guerau de Arellano, J., Hartogensis, O., Benedict, I., De Boer, H., Bosman, P., Botía, S., Cecchini, M. A., Faassen, K., González-Armas, R., Van Diepen, K., et al.: Advancing understanding of land–atmosphere interactions by breaking discipline and scale barriers, Annals of the New York Academy of Sciences, 1522, 74–97, 2023.

https://doi.org/10.5194/egusphere-2024-1519
Preprint. Discussion started: 24 May 2024

Várnai, T. and Davies, R.: Effects of cloud heterogeneities on shortwave radiation: Comparison of cloud-top variability and internal heterogeneity, Journal of the atmospheric sciences, 56, 4206–4224, 1999.

Wapler, K. and Mayer, B.: A fast three-dimensional approximation for the calculation of surface irradiance in large-eddy simulation models, Journal of Applied Meteorology and Climatology, 47, 3061–3071, 2008.

Wissmeier, U., Buras, R., and Mayer, B.: PaNTICA: A fast 3D radiative transfer scheme to calculate surface solar irradiance for NWP and LES models, Journal of Applied Meteorology and Climatology, 52, 1698–1715, https://doi.org/10.1175/JAMC-D-12-0227.1, 2013.

Witthuhn, J., Hünerbein, A., Filipitsch, F., Wacker, S., Meilinger, S., and Deneke, H.: Aerosol properties and aerosol-radiation interactions in clear-sky conditions over Germany, Atmospheric Chemistry and Physics, 21, 14 591–14 630, https://doi.org/10.5194/ACP-21-14591-2021, 2021.